



## Layer by Layer Silver Acetate based Coating on Glass and Cement Substrates to Tailor Reflectance and Conductance

Ghusoon M. Ali<sup>1\*</sup>, Maan S. Hassan<sup>2</sup>, Ehssan S. Hassan<sup>3</sup> & Mohammed O. Dawood<sup>3</sup>

<sup>1</sup>Electrical Engineering Department, College of Engineering, Mustansiriyah University, Bab Al Muadham, 10047, Baghdad, Iraq

<sup>2</sup>Civil Engineering Department, University of Technology, Al-Sinaa Street, 10066, Baghdad, Iraq

<sup>3</sup>Department of Physics, College of Science, Mustansiriyah University, Palestine Street, 10052, Baghdad, Iraq

\*E-mail:

### Highlights:

- Tailoring reflectivity and conductivity by layer assembly of organic silver thin film.
- Growing films over glass and cement substrates by sol-gel method with annealing at 100 °C.
- Eight-layer film has high reflectance and conductance features at room temperature.
- Multilayered thin film in general is thermally stable for annealing up to 400 °C.
- Multilayered film turns into an insulator when the annealing temperature reaches 500 °C.

**Abstract.** Tailoring reflectance and conductance was achieved through layer by layer assembly of a silver acetate based multilayer coating. The coating was applied over glass and cement substrates by sol-gel spin coating and by brush painting, respectively. The structural, optical and electrical characteristics and the composition of the coating were studied. The diffraction peaks for all films revealed that the face-centered cubic lattice of the silver crystal structure and the films with more layers had a higher degree of crystallinity. The optical characteristics showed that having more layers leads to decreasing transmittance and increasing reflectance. The I-V characteristics of all samples showed typical ohmic contacts in a voltage range of -1 to 1 V. The conductance increased drastically as the coating developed into multiple layers. The eight-layer coated glass and cement based substrates had very low surface resistance, at 4  $\Omega$  and 2  $\Omega$  at 1 V, respectively. The study also revealed that the resistance behavior of a multilayered film generally is thermally stable for annealing up to 400 °C. The coating resistance was significantly increased by further increasing the post-annealing beyond 500 °C. The studied multilayered coating can be used to tailor the reflectance and conductance of dielectric substrate surfaces for various optoelectronics and sensor device applications.

**Keywords:** *cement; coating; conductance; glass; reflectance introduction.*

---

Received November 14<sup>th</sup>, 2018, 1<sup>st</sup> Revision November 25<sup>th</sup>, 2019, 2<sup>nd</sup> Revision February 11<sup>th</sup>, 2020, Accepted for publication March 24<sup>th</sup>, 2020.

Copyright ©2020 Published by ITB Institute for Research and Community Services, ISSN: 2337-5779, DOI: 10.5614/j.eng.technol.sci.2020.52.2.8

## 1 Introduction

Conductive coatings have drawn significant research attention due to their potential application in electronic, optoelectronic and sensor devices. They can be applied for example in solar cells, displays, light-emitting diodes, sensors, photodetectors, and antennas [1]. Tin-doped indium oxide (ITO) is a typical conductive thin film coating, however, indium is a rare and expensive element. Silver (Ag) based conductive coatings are potentially an inexpensive alternative option [2]. Many techniques to deposit silver-based conductive coatings have been reported, such as vapor phase deposition [3], magnetron sputtering [4], pulsed laser deposition [5], spray pyrolysis [6], and sol-gel [7]. Among these, the sol-gel method has emerged as one of the most promising well-controlled low-cost processing routes [8]. Various coating techniques can be performed to deposit a sol-gel onto a substrate, such as dip-coating, spin-coating, brushing, and spraying [9]. There are many factors that affect the characteristics of a coating produced by the sol-gel method. These factors include coating technique used, substrate used (i.e. temperature, materials, roughness), the nature of the sol-gel (i.e. viscosity, drying rate, surface tension), and the number and thickness of the coated layers [10].

Typically, the conductive coating is applied to a dielectric substrate. Glass and cement based materials are still the main choices for construction in the 21st century [11]. In addition to the accumulated knowledge on their mechanical and dielectric properties, they also contribute to the aesthetics of buildings and save energy [12]. With the aim to convert building surfaces so they can generate power by integrating solar cells and/or to create self-sensing buildings, various strategies have been adopted. One method is using surface coating/engineering technology [13]. Conductive coatings play an essential role in the application of this technology.

Multilayered film coating structures can be optimized to tailor the resistivity and transparency of the film [14,15]. Previously, Khan, *et al.* [15] have investigated the electrical and optical properties of a multilayer ZnO thin film coating on glass substrates, finding that having more layers decreases the resistance and the optical band gap. Wu, *et al.* [14] explored the optical and electrical properties of multilayer thin films of silver mid-layer-embedded BaSnO<sub>3</sub> structures on polycarbonate substrates. They demonstrated that a higher thickness of the Ag mid-layer decreases the transmittance and resistance.

A review of the literature showed that the properties of silver-based multilayer coatings grown by sol-gel technique have not been investigated yet. The present study facilitates the fabrication of high conductive and reflective coatings at low temperature for optoelectronic and sensing applications at affordable cost.

Coatings were applied over glass and cement substrates by sol-gel spin coating and brush painting techniques, respectively. The structural, electrical, optical properties and thermal stability of the silver acetate based conductive coating were studied layer by layer (up to eight layers).

## 2 Experimental Methods and Materials

All chemicals were analytical grade reagents and employed without any additional purification. In preparation of the silver acetate based sol-gel for the conductive coating, 0.835 g silver acetate ( $\text{CH}_3\text{COOAg}$ ) was dissolved in 10 ml isopropanol ( $\text{C}_3\text{H}_8\text{O}$ ). The solution was stirred at room temperature until a white-colored solution was obtained. After that, the desired amount of diethanolamine [ $\text{HN}(\text{CH}_2\text{CH}_2\text{OH})_2$ , DEA] was added. The solution was found to change to a milky yellowish color. The molar ratio of DEA to silver acetate was 1 and the concentration of silver acetate was 0.5 M. acetic acid ( $\text{C}_2\text{H}_4\text{O}_2$ ) was added dropwise (0.5 ml) to the solution, which was then mixed. After 30 min of stirring at room temperature, a beige homogeneous thick solution was obtained. This solution was then used for coating. DEA was used as stabilizer and isopropyl alcohol as solvent. Acetic acid was used for fast decomposition of the deposited solution.

An adapted Tollens' reagent was used to prepare the silver-based sol-gel by a complexation reaction between silver acetate and diethanolamine [16,17]. Silver acetate is preferable as starting material because of its ability to produce a stable and nonexplosive silver precursor [16-18]. The silver acetate reacts with diethanolamine to create the diammine silver(I) acetate [ $\text{Ag}(\text{NH}_3)_2\text{OAc}$ ] (1) without the need for a silver oxide intermediate [18]. In order to obtain a fast decomposition regime, acetic acid was employed in the solution. The use of acetic acid followed by post-deposition heating to 100 °C results in the formation of carbon dioxide gas and water vapor, producing a free residual reducing agent [18]. The decomposition effect of acetic acid is the key factor, leading to transformation of the silver ions into silver crystals. This reaction increases the conductivity of the resulting thin film by improving the continuity of the silver particles [19]. The isopropyl alcohol solvent was removed by spin coating and heating the deposited thin film up to 100 °C.

Before the deposition process, 2.5 x 2.5 cm<sup>2</sup> soda lime glass (plain microscope slides) substrates were chemically cleaned using acetone, isopropanol, and deionized water. The films were deposited using the sol-gel spin coating technique. The solution (0.5 ml) was dropped onto the cleaned glass substrates, which were spun at a spin speed and a spin time of 2000 rpm and 40 sec, respectively. After this step, the coated substrates were heated in air at 100 °C for 10 min on a hotplate to evaporate the solvent and remove organic residues present

in the silver-based layer. The deposition procedures from coating to drying described above were repeated 1 to 7 times to obtain samples with 1 layer to 8 layers.

The prepared silver sol-gel was also utilized as a dye to coat selected faces of cementitious samples of 50-mm<sup>3</sup> cubic size to examine the use of the solution as a conductive paint. Ordinary Portland cement (OPC) type I, silica sand with a maximum size of 2.36 mm and water were the main materials used to fabricate the cementitious cubes of this research. The (OPC), with a Bogue composition of 58.80% C3S, 19.14% C2S, 7.95% C3A, and 9.42% C4AF, complied with the ASTM C150-15 standard specification. Mixing of the materials was performed according to ASTM C305. The cubes were demolded after 1 day of casting and then standard-cured in lime-saturated water for 28 days. After 28 days of curing, the samples were cleaned using deionized water. The cleaned samples were coated with an art paintbrush and then conditioned in an oven at 100 °C for 10 min. These painting and heating steps were repeated 7 times to obtain 1- to 8-layer samples. The oven drying duration for the final layer was increased to 30 min to make sure that the applied coating was completely dried and hardened on the rough surface. A gradual color change from black to white-grey was noticed with progressive drying during the layer-by-layer process.

The surface morphology of the glass coated samples was measured by using a scanning electron microscope (SEM), model FE-SEM, Tescan Vega III. The crystalline phase of the thin films was characterized by X-ray diffraction (XRD) using Cu K $\alpha$  radiation in the range 2 $\theta$  from 20° to 80°. UV-visible transmittance spectra were observed in the wavelength range of 200 to 900 nm using a UV-VIS-NIR spectrophotometer. Fourier transformation infrared spectroscopy (FTIR) was used to determine the chemical components and absorption bands of the prepared layer. The thickness of the silver-based coating was estimated to be in the range of about 1  $\mu$ m for one layer. The coated films' average thicknesses were ~0.9, 2.1, 3.3, 4.5, 5.4, 6.8, 7.9 and 9.8  $\mu$ m for 1 to 8 layers, respectively. The film thicknesses were estimated by a thin film TFProbe (Angstrom Advance Inc.).

For both sets (i.e. glass and cement based substrates), the conventional I-V characteristics of the coated films were measured at room temperature using a 4200-SCS semiconductor characterization system (Keithley) with an applied voltage range of -1 V to 1 V. In comparison with the rough cement-based substrate surface, the glass substrate had a very smooth surface; both substrates had a dielectric nature.

Two crocodile clips and two probes with copper wires were connected to the coated surface of the glass and cement substrates, respectively. The glass samples

were isochronally annealed from 100 °C to 500 °C in steps of 100 °C for 10 min to study the thermal stability. I-V characteristics measurements at room temperature followed each annealing cycle.

### 3 Results and Discussions

The surface morphology and the cross-section of the multilayer (8-layer) silver conductive coating on the glass substrate were investigated using SEM images. The SEM images are shown in Figure 1(a) and (b). Figure 1(a) shows that the sample surface contains dense closely packed particles with a broad size, varying from 50 nm to 1 µm. The particles were found to agglomerate in clusters, resulting in a granular surface. The cross-section SEM images of the 8-layer silver conductive coating show the film grown on the glass substrate. The layers were coupled together without boundaries between the layers. Figure 1(b) shows that the thickness of the 8-layer coating was around 10 µm.

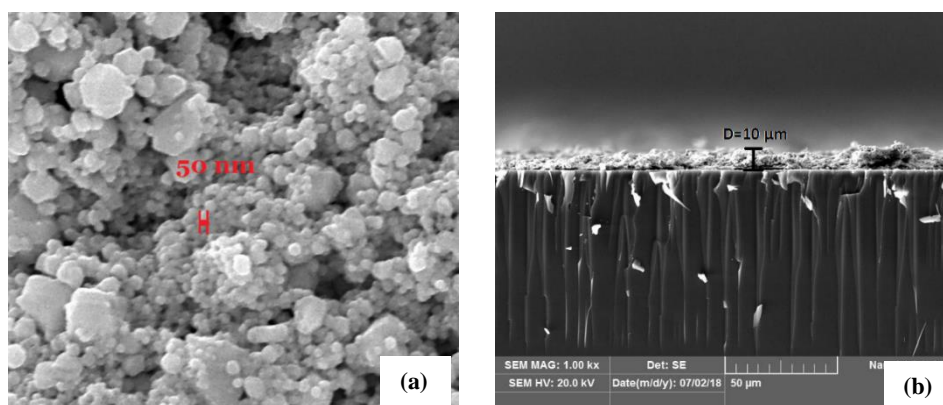


**Figure 1** SEM images of 8-layer silver conductive coating on glass substrate: (a) surface morphology image, and (b) cross-section image.

X-ray diffraction (XRD) measurements were performed at room temperature for the thin films deposited on glass substrate by spin coating and heated to 100 °C for 10 min. The XRD results revealed only the presence of silver peaks for all samples. Figure 2 shows the XRD patterns for the 2-layer, 4-layer, 6-layer and 8-layer films, with 2.1, 4.5, 6.8, and 9.8 µm average thickness, respectively.

The diffraction peaks of all films indicate the face-centered cubic lattice of an Ag crystal structure [20]. It can clearly be seen that the films with more layers had higher intensity and sharper peaks, which indicates a higher degree of crystallinity. The two silver peaks were present throughout all coated surfaces, appearing at  $2\theta$  from 20° to 60° at 38.1° and 44.3°, which corresponds to the

(111) and (200) directions, respectively. The average crystallite size was calculated by Debye–Scherrer’s equation:

$$D = \frac{K\lambda}{B \cos \theta} \quad (1)$$

where  $D$  is the crystallite size,  $K$  is the correction factor taken as 0.94 in the calculation,  $\lambda$  is the X-ray wavelength,  $B$  is the full width at half maximum of the X-ray peak, and  $\theta$  is Bragg’s angle. The crystalline size of the 2, 4, 6 and 8 layers was estimated at 15.74 nm, 17 nm, 19.21 nm and 21.39 nm, respectively.

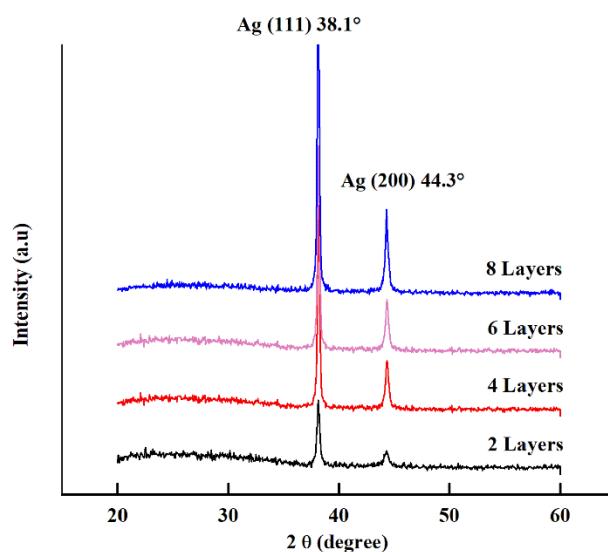


**Figure 2** X-ray diffraction patterns of silver-based conductive coating deposited by spin coating on glass substrate and heated at 100 °C for 10 min.

The Fourier transform infrared (FTIR) spectra of the thin films were recorded. Figure 3 shows the FTIR spectra of the double layer silver-based conductive coating as an example, since the FTIR spectra of all samples were almost identical. The figure shows only two peaks: one peak at  $555 \text{ cm}^{-1}$  is observed for Ag particulars due to Ag-O excitation [21, 22] and the other peak is due to the carbonate group observed at  $835 \text{ cm}^{-1}$  [23]. The FTIR spectra confirmed that there were no other residual groups.

Figure 4 shows the UV-visible transmittance spectra as a function of the number of layers of the silver based coating on the glass substrate. The absorption edge at 300 nm is due to absorption by the glass substrate. All studied silver based samples had maximum transmittance at a constant place in the 322 nm

wavelength, in agreement with other reports [24]. Generally, the figure demonstrates that the films with more layers had lower transmittance. As can be seen in Figure 4, the transmittance of the double-layer film decreased after reaching its maximum value (53%) at 322 nm down to the minimum value (8%) at 400 nm wavelength.

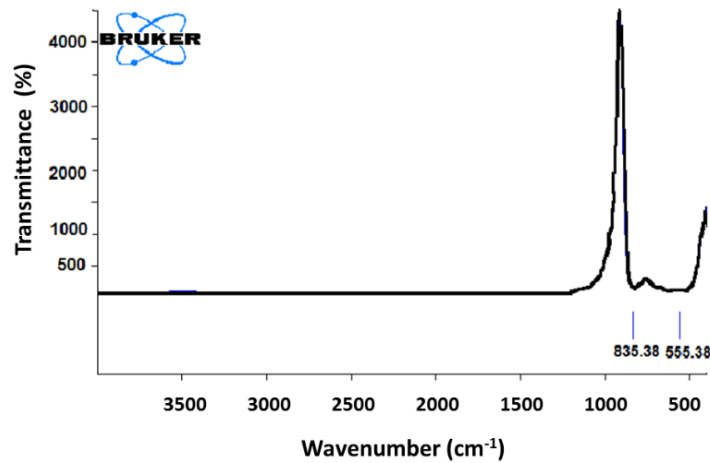


**Figure 3** FTIR spectra of double-layer silver-based conductive coating on glass substrate.

Beyond the minimum value, the transmission started to increase up to 20% in the visible and near IR region (400~900 nm wavelength). Regarding the 4-layer sample, the spectrum characteristics were quite similar to those of the 2-layer sample, with lower transmittance values of around 10%. For the 6-layer and 8-layer samples, the maximum transmittance decreased drastically (about 8%) as compared to the samples with fewer layers.

The transmittance in the range of 400~900 nm wavelength was 4% and 1% for the 6- and 8-layer films, respectively. The coating thickness decides the transmittance percentage; silver films with higher thickness usually exhibit less transparency [25]. The calculated value of the extinction coefficient ( $k$ ) and the refractive index ( $n$ ) was used to estimate the values of the reflectance of the material ( $R$ ) using the following equation:

$$R = \frac{(n-1)^2 + k^2}{(n+1)^2 + k^2} \quad (2)$$

The optical reflectance of double, four, six and eight layers of silver-based coating in the 300 to 900 nm wavelength range is plotted in Figure 5. This graph

shows that the reflectance increased remarkably with film thickness. The 2- and 4-layer samples had maximum reflectance somewhere at the 400 nm wavelength, while the maximum reflectance for the 6- and 8-layer films was at 350 nm. The reflectance decreased gradually in the range from 400 to 900 nm wavelength for the 2- and 4-layer films.

The reflectance of the two-layer sample decreased by 20% from 0.85 at 400 nm wavelength to 0.65 at 900 nm wavelength. For the 6- and 8-layer samples, the reflectance was almost constant in the range from 350 to 900 nm wavelength, after reaching their maximum values of 0.93 and 0.99, respectively. This means that they were 93% and 99% higher than the incident radiation.

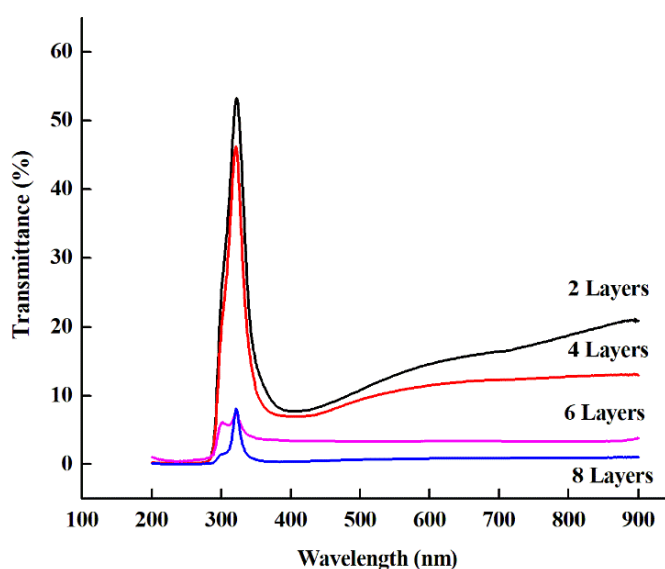


**Figure 4** UV-visible transmittance spectra as a function of the number of layers of silver-based coating on glass substrate.

Falling were reflected as compared to the total light absorbed and transmitted in this wavelength range. The 8-layer film's reflectance was about equal to the reflectance of a bulk slab of Ag 99% across the visible spectrum. Increasing the number of coated layers means increasing the Ag loaded in the film, which leads to a decrease of transmittance and an increase of reflectance. With such high reflectance, the studied multilayered coated films act as a mirror reflector, which can effectively reflect untransmitted or unabsorbed light. This reflection benefits the application of silver coatings in various optoelectronic devices, such as solar cells and photodetectors. The benefit gained from using high-reflectance thin film



on the backside of an optoelectronic device is to make the optical energy run through the active layer again [26,27].

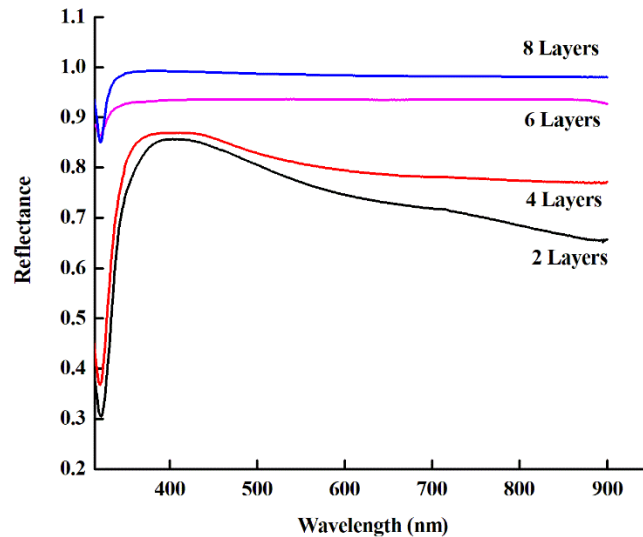


**Figure 5** Optical reflectance spectra as a function of the number of layers of silver-based coating on glass substrate.

I-V measurements of the silver-film coated glass were carried out with two crocodile clips and a metal wire, using a Keithley 4200-SCS in the air at room temperature. Figure 6 demonstrates the I-V characteristics of the films with 2 to 8 layers in step 2. The samples with 4 to 8 layers showed a typical ohmic contact in the voltage range from -1 to 1 V. For one to three layers, the current showed fluctuations in the range of fractions of a microampere.

The value of the current increased significantly for four layers as compared to a lower number of layers. The current was in the range of milliamperes (97.1 mA) at an applied voltage of 1 V. From linear fitting of the curve, the average resistance was found to be 1021  $\Omega$ . The decrement in surface resistance is attributed to the transition from isolated island silver particles to larger three-dimensional interconnected clusters according to the Volmer-Weber growth mechanism [28]. The electrical resistance of the films further decreased with an increase in film thickness. The resistance for 6 and 8 layers was about 21.9  $\Omega$  and 4  $\Omega$ , respectively. Since the silver particle clusters continue to accumulate, a complete continuous conduit is formed as the thickness increases.

The resistance values for the coated samples with 4, 6 and 8 layers were confirmed by using a precise Avometer. Figure 7 shows the dependence of the conductance on the thickness of the silver-based coating. The conductance properties of this type of silver-based conductive coatings are decided by the embedded silver particles [3]. The silver film can be illustrated as a system of silver particles – islands implanted in a combined organic medium on a substrate and a minuscule spacing between particles.

Figure 7 shows that the electrical conductance of the studied films can be divided into three stages. The first stage is the dielectric stage. Because of the discontinuous isolated discrete particles, the 2-layer coating exhibits a very low conductance, in the order of  $10^{-7}$  S. The second stage is the transition stage. As the film thickness increases (four layers), the electrical conductance enhances sharply, up to three orders of magnitude, and becomes about  $10^{-4}$  S. This enhancement is due to the coalescence of the isolated particles. The last stage is the metallic stage. When the film thickness is further increased, the film comes closer and closer to metallic conductance. The conductance for 6 and 8 layers further increased, to 0.04 S and 0.24 S, respectively. The silver decomposition multilayer thin films' performance is rated in Table 1.

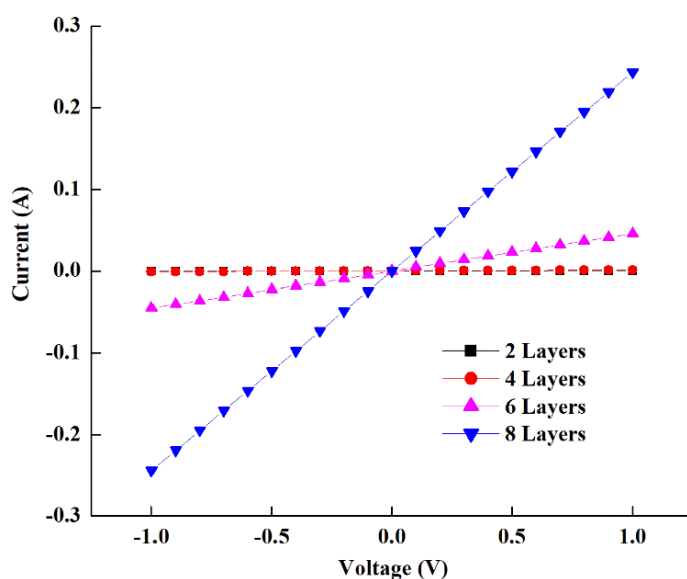


**Figure 6** I-V characteristics of silver-based coating on glass substrate as a function of the number of layers.

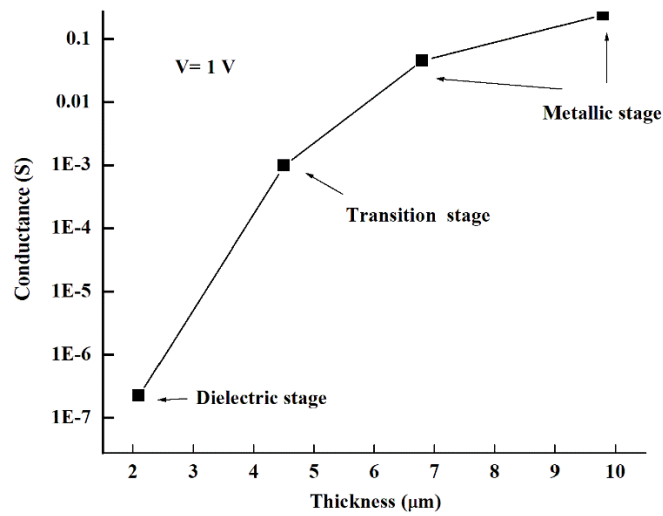


**Figure 7** Conductance as a function of silver-based coating thickness on glass substrate.

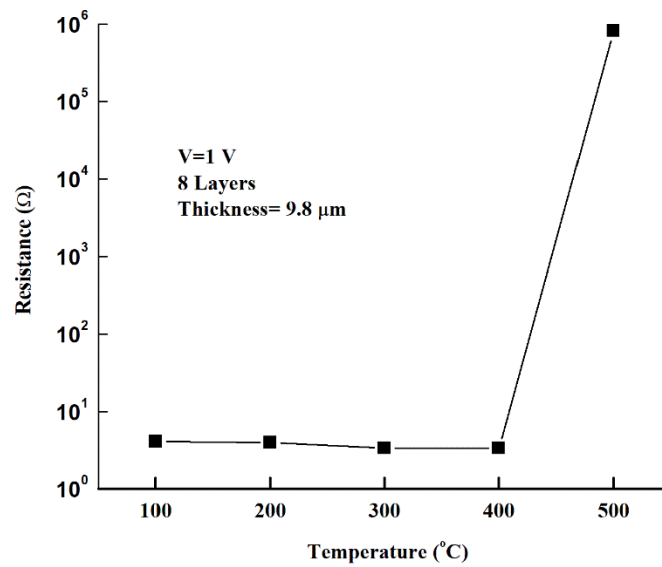


**Figure 8** Resistance as a function of the temperature of the silver-based conductive coating.

**Table 1** Performance rating of silver multilayer coating on glass substrate.

No. of layers	Crystallite size (nm)	Thickness ( $\mu\text{m}$ )	Reflectance (%) @ 400nm	Transmittance (%) @ 400nm	Resistance ( $\Omega$ ) @ 1V
2 layers	15.74	2.1	85.628	7.73184	4.4843E6
4 layers	17	4.5	86.936	6.98786	1029
6 layers	19.21	6.8	93.427	3.39255	21.9
8 layers	21.39	9.8	99.235	0.38588	4.1

In order to study the thermal stability of the eight-layer conductive film coated glass, I-V measurements were carried out at room temperature after different annealing treatments of the samples. The films were annealed for 10 min in a temperature range of 100 to 500 °C under ambient air. The values of resistance were estimated from the I-V measurements as shown in Figure 8.

The resistance decreased slightly to an annealing temperature of 400 °C. The resistance decreased from 4.1  $\Omega$  at 100 °C to 3.3  $\Omega$  at 400 °C. This decrement in resistance is attributed to merging of the silver particles in the coated film. The resistance reached its maximum value after annealing at a temperature of 500 °C. The resistance became  $8 \times 10^5 \Omega$  at 500 °C and the studied film tended to behave more like an insulator, as can be seen in Figure 8. A significant transformation in the resistivity confirms that the annealing changes the thin film structure to a significant extent [29]. Due to interactions between silver and oxygen at high temperature, new phases appear [30].

To assess the conductive coating on a rough surface, the films were also grown over cement substrates by artbrush coating. Each coating layer was annealed at 100 °C for 10 min. I-V measurement of the conductive paint coated cement specimens was carried out, with two probes with metal wire, using a Keithley 4200-SCS in the air at room temperature (not shown). Similar to the conductive coating on glass substrate, the surface of the coated cement started showing typical ohmic behavior when the number of layers was equal to 4 or higher. A lower number of layers gave some fluctuation in the current values, in the range of microamperes.

The 2, 4, 6 and 8 coating layers on cement substrate had a resistance of 800 k, 869.5, 25.25 and 2.27  $\Omega$ , respectively, at 1V. The resistance decrease is due to the accumulation of silver particle clusters, creating a complete and continuous path to the electrons. As with the multilayer conductive coated glass, the values of the resistance of the conductive coated cement were confirmed by using precise Avometer.

To compare and contrast the I-V characteristics of the silver-based coatings on glass and cement based substrates, Figure 9 was plotted. It can clearly be seen from the I-V plot that both 8-layer surfaces had very low resistance,  $4 \Omega$  and  $2 \Omega$  at 1 V for the glass- and the cement-based substrate, respectively. The slightly higher conductance of the silver-based coating on cement-based substrate is attributed to the coating technique and the cement-based substrate's rough surface. The brush coating loaded more material on the rough cement-based substrate than the spin coating did on the smooth glass substrate. More silver-based film material means more conductivity, as we concluded in the previous discussions. The brush coating technique is more convenient for a cement-based substrate than the spin coating technique due to its bulky size and the rough surface of the cubic cement-based substrate.

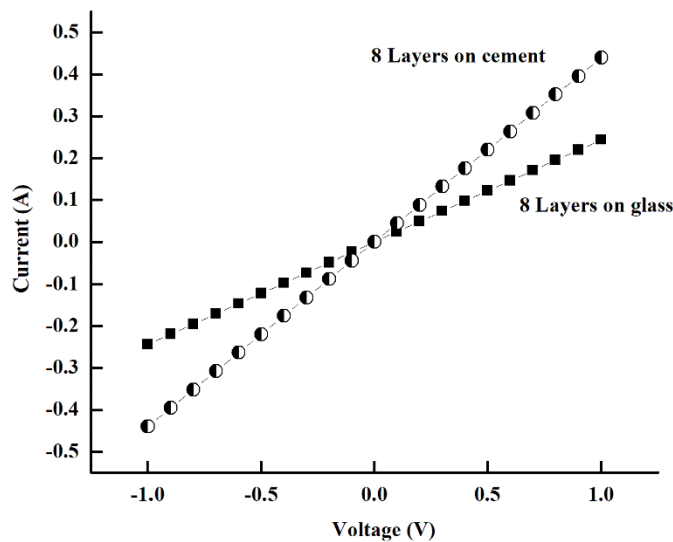


**Figure 9** I-V characteristics of eight-layer silver-based coating on glass and cement based substrates.

#### 4 Conclusions

Tailoring the reflectance and conductance of layer by layer silver acetate based sol-gel coating was investigated. Two different deposition techniques were used: spin coating on glass substrate and artbrush paint coating on cement-based substrate. The synthesis of silver sol-gel deposition showed that acetic acid is the key factor in improving the coating's conductance due to the transformation of silver ions to silver crystal. It was revealed that the reflectance of the coated glass samples increased remarkably with an increase in the number of film layers until

reaching silver bulk reflectance. With such high reflectance, multilayered coated films can act as a mirror reflector that can effectively reflect light. The I-V characteristics of both samples on glass-based and cement-based substrates showed that the multilayered thin film's behavior obeyed Ohm's law. The conductance increased significantly with film thickness. The results show three distinctive conductance behaviors: dielectric, transition, and metallic behavior. The multilayer coated glass- and cement-based substrates (8 layers) provided a very low surface resistance of 4  $\Omega$  and 2  $\Omega$  respectively at 1 V. The slightly lower resistance of a silver-based coating on cement-based substrate is attributed to the coating technique and the high roughness of the surface.

The brush coating technique loaded more material onto the cement-based substrate than the spin coating did onto the glass substrate. More silver-based coating material means higher conductivity. This study also revealed that the resistance performance of the multilayered coating was in general thermally stable for annealing up to 400 °C. The coating's resistance increased significantly and the film showed insulator behavior as the annealing temperature was increased to 500 °C, which is attributed to the appearance of a new phase of the material. The studied multilayered coating can be deployed as a cost-effective, easy-to-fabricate solution with tailored reflectance and conductance of the dielectric substrate surface for various optoelectronics and sensors device applications.

### Acknowledgements

The authors would like to acknowledge the Microelectronics Lab of the Electrical Engineering Department, College of Engineering, Mustansiriyah University, and the Concrete Lab of the Civil Engineering Department, University of Technology for their technical assistance. This research did not receive any specific grant from funding agencies in the public, commercial, or not-for-profit sectors.

### References

- [1] Riza, M.A., *Prospects and Challenges of Perovskite Type Transparent Conductive Oxides in Photovoltaic Applications. Part I Material Developments*, Sol. Energy, **137**, pp. 371-378, 2016.
- [2] Kou, P., Yang, L., Chi, K. & He, S., *Large-Area and Uniform Transparent Electrodes Fabricated by Polymethylmethacrylate-assisted Spin-Coating of Silver Nanowires on Rigid and Flexible Substrates*, Opt. Mater. Express, **5**(10), pp. 2347-2358, 2015.
- [3] Wei, H. & Eilers, H., *From Silver Nanoparticles to Thin Films: Evolution of Microstructure and Electrical Conduction on Glass Substrates*, J. Phys. Chem. Solids, **70**(2), pp. 459-465, 2009.

- [4] Maréchal, N., Quesnel, E. & Pauleau, Y., *Silver Thin Films Deposited by Magnetron Sputtering*, *Thin Solid Films*, **241**(1-2), pp. 34-38, 1994.
- [5] Fazio, E., Neri, F., Ponterio, R.C., Trusso, S., Tommasini, M. & Ossi, P. M., *Laser Controlled Synthesis of Noble Metal Nanoparticle Arrays for Low Concentration Molecule Recognition*, *Micromachines*, **5**(4), pp. 1296-1309, 2014.
- [6] Morales, J., Sánchez, L., Martín, F., Ramos-Barrado, J.R. & Sánchez, M., *Synthesis, Characterization, and Electrochemical Properties of Nanocrystalline Silver Thin Films Obtained by Spray Pyrolysis*, *J. Electrochem. Soc.*, **151**(1), pp. A151-A157, 2004.
- [7] Schneid, A.C., *Silver Nanoparticle Thin Films Deposited on Glass Surface Using an Ionic Silsesquioxane as Stabilizer and as Crosslinking Agent*, *J. Braz. Chem. Soc.*, **26**(5), pp. 1004-1012, 2015.
- [8] Bahuguna, G., Mishra, N.K., Chaudhary, P., Kumar, A. & Singh, R., *Thin Film Coating through Sol-Gel Technique*, *Res. J. Chem. Sci.*, **6**(7), pp. 65-72, 2016.
- [9] Rout, T., Bera, S., Udayabhanu, G. & Narayan, R., *Methodologies of Application of Sol-Gel Based Solution Onto Substrate: A Review*, *J. Coat. Sci. Technol.*, **3**(1), pp. 9-22, 2016.
- [10] Tyona, M. D., *A Theoretical Study on Spin Coating Technique*, *Adv. Mater. Res.*, **2**(4), pp. 195-208, 2013.
- [11] Brauer, D. S., Gentleman, E., Farrar, D. F., Stevens, M.M. & Hill, R.G., *Benefits and Drawbacks of Zinc in Glass Ionomer Bone Cements*, *Biomed. Mater.*, **6**(4), 045007, 2011.
- [12] Hosseini, T., Flores-Vivian, I., Sobolev, K. & Kouklin, N., *Concrete Embedded Dye-Synthesized Photovoltaic Solar Cell*, *Sci. Rep.*, **3**, pp. 1-5, 2013.
- [13] Gherardi, F., *Efficient Self-Cleaning Treatments for Built Heritage Based on Highly Photo-active and Well-dispersible TiO<sub>2</sub> Nanocrystals*, *Microchem. J.*, **126**, pp. 54-62, 2016.
- [14] Wu, M., Yu, S., He, L., Yang, L. & Zhang, W., *High Quality Transparent Conductive Ag-Based Barium Stannate Multilayer Flexible Thin Films*, *Sci. Rep.*, **7**(1), pp. 1-9, 2017.
- [15] Khan, M.I., Bhatti, K.A., Qindeel, R., Alonizan, N. & Althobaiti, H.S., *Characterizations of Multilayer ZnO Thin Films Deposited by Sol-Gel Spin Coating Technique*, *Results Phys.*, **7**, pp. 651-655, 2017.
- [16] Yang, W., Liu, C., Zhang, Z., Liu, Y. & Nie, S., *One Step Synthesis of Uniform Organic Silver Ink Drawing Directly on Paper Substrates*, *J. Mater. Chem.*, **22**(43), pp. 23012-23016, 2012.
- [17] Yoon, H., Kim, S.W., Chun, S.K., Lee, D.W., Kim, S.W. & Kwon, W.J., *Organic Silver Complex Compound Used in Paste for Conductive Pattern Forming*, US patent, 0021704 A1, 2010.

- [18] Walker, S.B. & Lewis, J.A., *Reactive Silver Inks for Patterning High-Conductivity Features at Mild Temperatures*, J. Am. Chem. Soc., **134**(3), pp. 1419-1421, 2012.
- [19] Dong, Y., *Optimizing Formulations of Silver Organic Decomposition Ink for Producing Highly-Conductive Features on Flexible Substrates: The Case Study of Amines*, Thin Solid Films, **616**, pp. 635-642, 2016.
- [20] Vaseem, M., Lee, S.K., Kim, J.G. & Hahn, Y.B., *Silver-Ethanolamine-Formate Complex Based Transparent and Stable Ink: Electrical Assessment with Microwave Plasma vs Thermal Sintering*, Chem. Eng. J., **306**, pp. 796-805, 2016.
- [21] Hussain, M.A., *One Pot Light Assisted Green Synthesis, Storage and Antimicrobial Activity of Dextran Stabilized Silver Nanoparticles*, J. Nanobiotechnology, **12**(1), Article No. 53, 2014.
- [22] Muhammad, G., *Glucuronoxylan-Mediated Silver Nanoparticles: Green Synthesis, Antimicrobial and Wound Healing Applications*, RSC Adv., **7**(68), pp. 42900-42908, 2017.
- [23] Kaleva, A., *Dissolution-Induced Nanowire Synthesis on Hot-Dip Galvanized Surface in Supercritical Carbon Dioxide*, Nanomaterials, **7**(7), Article No. 181, 2017.
- [24] Axelevitch, A., Gorenstein, B. & Golan, G., *Investigation of Optical Transmission in Thin Metal Films*, Phys. Procedia, **32**, pp. 1-13, 2012.
- [25] De, S., *Silver Nanowire Networks as Flexible, Transparent, Conducting Films: Extremely High DC to Optical Conductivity Ratios*, ACS Nano, **3**(7), pp. 1767-1774, 2009.
- [26] Hungerford, C.D. & Fauchet, P.M., *Design of a Plasmonic Back Reflector Using Ag Nanoparticles with a Mirror Support for an A-Si:H Solar Cell*, AIP Adv., **7**(7), 075004, 2017.
- [27] Liu, C.H. & Yu, X., *Silver Nanowire-Based Transparent, Flexible, and Conductive Thin Film*, Nanoscale Res. Lett., **6**(1), Article No. 75, 2011.
- [28] Logeeswaran, V.J., *Ultrasoother Silver Thin Films Deposited with A Germanium Nucleation Layer*, Nano Lett., **9**(1), pp. 178-182, 2009.
- [29] Nie, X., Wang, H. & Zou, J., *Inkjet Printing of Silver Citrate Conductive Ink on PET Substrate*, Appl. Surf. Sci., **261**, pp. 554-560, 2012.
- [30] Lavrenko, V.A., Malyshevskaya, A.I., Kuznetsova, L.I., Litvinenko, V.F. & Pavlikov, V.N., *Features of High-Temperature Oxidation in Air of Silver and Alloy Ag-Cu, and Adsorption of Oxygen on Silver*, Powder Metall. Met. Ceram, **45**(451), pp. 476-480, 2006.